

## Magnetic properties and magnetocaloric effects in $R_3Ni_2$ ( $R=Ho$ and $Er$ ) compounds

Q. Y. Dong, J. Chen, J. Shen, J. R. Sun, and B. G. Shen

Citation: *Appl. Phys. Lett.* **99**, 132504 (2011); doi: 10.1063/1.3643142

View online: <http://dx.doi.org/10.1063/1.3643142>

View Table of Contents: <http://apl.aip.org/resource/1/APPLAB/v99/i13>

Published by the [American Institute of Physics](http://www.aip.org).

---

### Related Articles

Magnetocaloric effect and its implementation in critical behavior study of  $Mn_4FeGe_{3x}Six$  intermetallic compounds

*J. Appl. Phys.* **110**, 113915 (2011)

Enhanced refrigerant capacity and magnetic entropy flattening using a two-amorphous  $FeZrB(Cu)$  composite

*Appl. Phys. Lett.* **99**, 232501 (2011)

Cooling field and temperature dependence on training effect in  $NiFe_2O_4$ - $NiO$  nanogranular system

*J. Appl. Phys.* **110**, 103902 (2011)

Composition dependent-magnetocaloric effect and low room-temperature coefficient of resistivity study of iron-based antiperovskite compounds  $Sn_{1x}GaxCFe_3$  ( $0 \leq x \leq 1.0$ )

*Appl. Phys. Lett.* **99**, 172503 (2011)

Effect of Fe substitution on magnetic and magnetocaloric effect in  $Gd(Co_{1-x}Fe_x)_2B_2$  compounds

*J. Appl. Phys.* **110**, 083915 (2011)

---

### Additional information on *Appl. Phys. Lett.*

Journal Homepage: <http://apl.aip.org/>

Journal Information: [http://apl.aip.org/about/about\\_the\\_journal](http://apl.aip.org/about/about_the_journal)

Top downloads: [http://apl.aip.org/features/most\\_downloaded](http://apl.aip.org/features/most_downloaded)

Information for Authors: <http://apl.aip.org/authors>

### ADVERTISEMENT

The logo for AIP Advances features the text 'AIP Advances' in a blue and green font. Above the text is a decorative graphic of several orange and yellow circles of varying sizes, arranged in a curved path that suggests a trail or a sequence of events.

*Submit Now*

Explore AIP's new  
open-access journal

- Article-level metrics now available
- Join the conversation! Rate & comment on articles

## Magnetic properties and magnetocaloric effects in $R_3\text{Ni}_2$ ( $R = \text{Ho}$ and $\text{Er}$ ) compounds

Q. Y. Dong,<sup>1,2,a)</sup> J. Chen,<sup>2</sup> J. Shen,<sup>2,3</sup> J. R. Sun,<sup>2</sup> and B. G. Shen<sup>2</sup>

<sup>1</sup>Department of Physics, Capital Normal University, Beijing 100048, People's Republic of China

<sup>2</sup>State Key Laboratory for Magnetism, Institute of Physics, Chinese Academy of Sciences, Beijing 100190, People's Republic of China

<sup>3</sup>Technical Institute of Physics and Chemistry, Chinese Academy of Sciences, Beijing 100190, People's Republic of China

(Received 7 July 2011; accepted 3 September 2011; published online 26 September 2011)

Magnetic and magnetocaloric properties of  $R_3\text{Ni}_2$  ( $R = \text{Ho}$  and  $\text{Er}$ ) compounds have been investigated. Both  $\text{Ho}_3\text{Ni}_2$  and  $\text{Er}_3\text{Ni}_2$  compounds undergo two successive phase transitions: spin reorientation transition and second-order ferromagnetic-paramagnetic transition. The maximal values of magnetic entropy change are achieved to be  $21.7 \text{ J kg}^{-1} \text{ K}^{-1}$  for  $\text{Ho}_3\text{Ni}_2$  and  $19.5 \text{ J kg}^{-1} \text{ K}^{-1}$  for  $\text{Er}_3\text{Ni}_2$  for a field change of 0-5 T. A large refrigerant capacity (RC) of  $496 \text{ J kg}^{-1}$  in the composite material is also obtained. Large reversible magnetocaloric effect and RC indicate the potentiality of  $R_3\text{Ni}_2$  ( $R = \text{Ho}$  and  $\text{Er}$ ) compounds as candidates for low-temperature magnetic refrigerant. © 2011 American Institute of Physics. [doi:10.1063/1.3643142]

Magnetic refrigeration based on magnetocaloric effect (MCE) of solid-state working substances has been widely employed in ultra-low temperature.<sup>1,2</sup> Recently, it has been anticipated to be a promising alternative technology available at high temperature and even room temperature, due to its higher energy-efficient and environment-friendly features as compared with the common gas-compression refrigeration technology that is used currently.<sup>3,4</sup> Large isothermal magnetic entropy change ( $\Delta S$ ), as an important parameter for evaluating the amount of the MCE, has been found in materials with a first-order or second-order phase transition, such as  $\text{Gd}_5(\text{Si}, \text{Ge})_4$ ,<sup>5</sup>  $\text{La}(\text{Fe}, \text{Si})_{13}$ ,<sup>6,7</sup>  $\text{MnAs}$ ,<sup>8,9</sup>  $\text{MnFe}(\text{P}, \text{As})$ ,<sup>10</sup>  $\text{Ni}_2\text{MnGa}$ ,<sup>11</sup> and  $\text{Gd}$ .<sup>4</sup> Researches are still in progress for exploring new materials which have large MCE at low fields near room temperature for the refrigeration technological application. However, systems exhibiting large MCE at low temperature are also important for basic research as well as special technological applications such as space science and liquefaction of hydrogen in fuel industry.<sup>3,4</sup> Therefore, it is desirable to explore magnetocaloric materials applicable in the low temperature range.

It was found that only rare earth atoms carry out magnetic moment, whereas Ni atoms remain nonmagnetic in the intermetallic compounds  $R_3\text{Ni}$  and  $R\text{Ni}$  series ( $R$  is heavy rare earth) with different crystal structure.<sup>12,13</sup>  $\text{Ho}_3\text{Ni}$  and  $\text{Er}_3\text{Ni}$  compounds crystallize in the orthorhombic  $\text{Fe}_3\text{C}$ -type structure. The compounds  $\text{HoNi}$  and  $\text{ErNi}$  crystallize in the orthorhombic  $\text{FeB}$ -type structure. The magnetic properties of two series have been investigated in detail. The  $\text{Er}_3\text{Ni}$  compound exhibits an antiferromagnetic (AFM) state below Néel temperature  $T_N$  ( $=7 \text{ K}$ ). The spin freezing phenomenon occurs in the temperature range between  $T_N$  and spin freezing temperature  $T_{\text{sf}}$  ( $=12 \text{ K}$ ).<sup>12</sup> The similar situation has been observed in  $\text{Ho}_3\text{Ni}$  compound with  $T_N = 15.5 \text{ K}$  and  $T_{\text{sf}} = 34 \text{ K}$ .<sup>12</sup> However, the  $\text{HoNi}$  and  $\text{ErNi}$  compounds display ferromagnetic (FM) state below their respective Curie temperature  $T_C$ . A noncollinear arrangement of magnetic

moment in rare earth sublattices has been confirmed. Moreover,  $\text{HoNi}$  and  $\text{ErNi}$  compounds have different arrangement of moments.<sup>13,14</sup> In one word,  $R_3\text{Ni}$  and  $R\text{Ni}$  series with  $R = \text{Ho}, \text{Er}$  have complicated magnetic structures.

The  $R_3\text{Ni}_2$  series ( $R = \text{Ho}$  and  $\text{Er}$ ) are the only kind of compounds between  $R_3\text{Ni}$  and  $R\text{Ni}$  series with  $R = \text{Ho}, \text{Er}$ . The crystalline structure of  $\text{Er}_3\text{Ni}_2$  is rhomb-centered rhombohedral (space group  $R\bar{3}$ ).<sup>15</sup> Er atoms occupy three nonequivalent sites, 3b site for Er(1), 6c site for Er(2), and 18f site for Er(3). Although Ni atoms also occupy 18f site, their positions are different from those of Er(3). The high-temperature phase of  $\text{Ho}_3\text{Ni}_2$  is isotypic with  $\text{Er}_3\text{Ni}_2$ .<sup>16</sup> Based on their complicated crystalline structure,  $\text{Ho}_3\text{Ni}_2$  and  $\text{Er}_3\text{Ni}_2$  compounds may have interesting magnetic structure. Large MCEs in them can be also expected due to the large rare earth content. Nevertheless, no reports on magnetic properties and MCEs of  $R_3\text{Ni}_2$  ( $R = \text{Ho}$  and  $\text{Er}$ ) compounds are found up to now. So in this paper, we present a study on the magnetic properties and MCEs of  $R_3\text{Ni}_2$  ( $R = \text{Ho}$  and  $\text{Er}$ ) compounds.

The samples were prepared by arc melting the constituent elements with the purity better than 99.9% in high-purity argon atmosphere. The obtained ingots were sealed in a high-vacuum quartz tube, annealed at 1023 K for 3 days for  $\text{Er}_3\text{Ni}_2$  and 873 K for 30 days for  $\text{Ho}_3\text{Ni}_2$ , and then quenched into liquid nitrogen. Powder x-ray diffractometer was performed to characterize the crystal structure of the samples. Magnetic measurements were carried out on a commercial MPMS-7 superconducting quantum interference device magnetometer. Heat capacity was measured by using a commercial PPMS-14H physical property measurement system.

Figure 1 shows the Rietveld refined powder x-ray diffraction patterns of  $R_3\text{Ni}_2$  ( $R = \text{Ho}$  and  $\text{Er}$ ) compounds. Almost all the diffraction peaks can be indexed to a rhomb-centered rhombohedral  $\text{Er}_3\text{Ni}_2$ -type structure. The lattice parameters obtained from the refinement are  $a = 8.523(5) \text{ \AA}$  and  $c = 15.758(6) \text{ \AA}$  for  $\text{Ho}_3\text{Ni}_2$  compound,  $a = 8.486(0) \text{ \AA}$  and  $c = 15.704(1) \text{ \AA}$  for  $\text{Er}_3\text{Ni}_2$  compound, which almost accord with the previous reports.<sup>15,16</sup>

<sup>a)</sup>Electronic mail: happylaugh746@gmail.com.

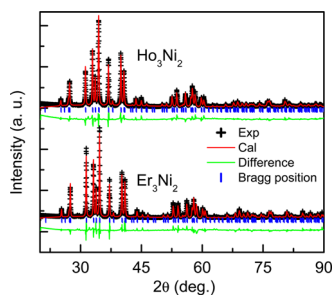


FIG. 1. (Color online) Rietveld refined powder XRD patterns of  $\text{Ho}_3\text{Ni}_2$  and  $\text{Er}_3\text{Ni}_2$  at room temperature. The observed data are indicated by crosses, and the calculated profile is the continuous line overlying them. The short vertical lines indicate the angular positions of the Bragg peaks of  $\text{Ho}_3\text{Ni}_2$  and  $\text{Er}_3\text{Ni}_2$ . The lower curve shows the difference between the observed and calculated intensity.

The low-field temperature-dependence of magnetization has been measured in order to determine magnetic state, phase transition temperature, and the nature of the transition. Figures 2(a) and 2(b) display the zero-field cooling (ZFC) and field-cooling (FC) magnetization curves of  $R_3\text{Ni}_2$  ( $R = \text{Ho}$  and  $\text{Er}$ ) compounds under a field of 0.01 T, respectively. It is found that there are two successive magnetic transitions in the  $M$ - $T$  curves for these compounds. For  $\text{Er}_3\text{Ni}_2$  compound (see Fig. 2(b)), the anomaly at low temperature may be a spin-reorientation (SR) transition. The SR transition temperature,  $T_{\text{SR}}$ , is decided to be  $\sim 12$  K. The authentic evidence needs to be supplied by neutron diffraction study in the future work. The transition at higher temperature corresponds to a change from FM to paramagnetic (PM) state with increasing temperature. The Curie temperature  $T_{\text{C}}$ , corresponding to the maximum slope of  $M$ - $T$  curve under a field of 0.01 T, is determined to be 17 K. The reciprocal magnetic susceptibility  $\chi^{-1}$  versus temperature for  $\text{Er}_3\text{Ni}_2$  under a field of 2 T is shown in the inset of Fig. 2(b). The magnetic susceptibility above 50 K obeys the Curie-Weiss law, and a positive PM Curie temperature is obtained, further confirming that a FM-PM phase transition takes place around  $T_{\text{C}}$  for  $\text{Er}_3\text{Ni}_2$ . It can be also seen from Fig. 2(b) that the ZFC and FC curves are completely reversible around  $T_{\text{C}}$ , which is a characteristic of a second-order transition.  $\text{Ho}_3\text{Ni}_2$  compound shows similar phenomena, as shown in Fig. 2(a) and its inset.  $T_{\text{SR}}$  and  $T_{\text{C}}$  are decided to be 10 K and 36 K, respectively.

Given that Ni atoms are nonmagnetic in  $R_3\text{Ni}_2$  ( $R = \text{Ho}$  and  $\text{Er}$ ) compounds, the effective magnetic moments per  $R$  atom of  $R_3\text{Ni}_2$  ( $R = \text{Ho}$  and  $\text{Er}$ ) compounds, evaluated from the slope of  $1/\chi$  in the PM region under the field of 2 T (see the insets of Figs. 2(a) and 2(b)), equal to  $10.9 \mu_{\text{B}}$  and  $9.9 \mu_{\text{B}}$ , which are close to the free ion values ( $10.6 \mu_{\text{B}}$  for Ho ion and  $9.5 \mu_{\text{B}}$  for Er ion), respectively. This illustrates that the hypothesis about the non-magnetism of Ni atoms in  $R_3\text{Ni}_2$  ( $R = \text{Ho}$  and  $\text{Er}$ ) compounds is correct, which is similar to the case in  $R_3\text{Ni}$  and  $R\text{Ni}$  compounds.<sup>12,13</sup> The PM Curie temperatures obtained by fitting the susceptibility data under the field of 2 T are 33 K and 18 K for  $\text{Ho}_3\text{Ni}_2$  and  $\text{Er}_3\text{Ni}_2$  compounds, respectively.

The isothermal magnetization curves as a function of magnetic field for  $R_3\text{Ni}_2$  ( $R = \text{Ho}$  and  $\text{Er}$ ) compounds were measured in applied fields of up to 5 T in a wide temperature range. Fig. 3(a) shows the typical magnetization curves of

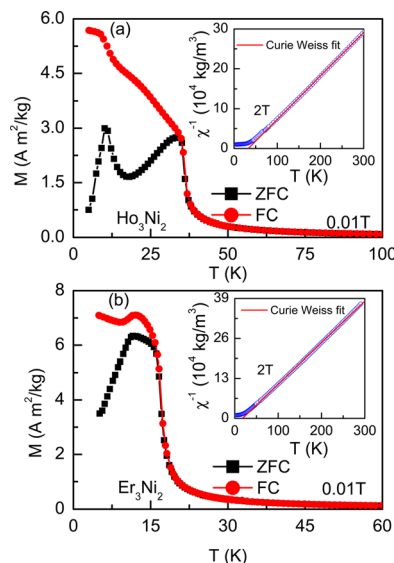


FIG. 2. (Color online) Temperature dependences of ZFC and FC magnetizations of  $\text{Ho}_3\text{Ni}_2$  (a) and  $\text{Er}_3\text{Ni}_2$  (b) under 0.01 T. The insets of (a) and (b) show the temperature variations of the ZFC inverse susceptibility fitted to the Curie-Weiss law under 2 T for  $\text{Ho}_3\text{Ni}_2$  and  $\text{Er}_3\text{Ni}_2$ , respectively.

$\text{Ho}_3\text{Ni}_2$  in the temperature range of 5-41 K. It can be seen from Fig. 3(a) that there is a considerable difference in the  $M$ - $H$  characteristics in different temperature ranges. The  $\text{Ho}_3\text{Ni}_2$  compound shows a metamagnetic transition at about 3.2 T below 17 K, whereas it shows typical FM nature in the temperature range of 17-35 K. The selective isothermal magnetization curves of  $\text{Er}_3\text{Ni}_2$  compound in the temperature range of 5-24 K are presented in Fig. 3(b). One can find that the  $\text{Er}_3\text{Ni}_2$  exhibits typical FM nature at temperatures lower than  $T_{\text{C}}$ . The Arrott plots<sup>17</sup> around  $T_{\text{C}}$  for  $R_3\text{Ni}_2$  ( $R = \text{Ho}$  and  $\text{Er}$ ) compounds are shown in the insets of Figs. 3(a) and 3(b), respectively. The positive slope of the Arrott plots confirms a characteristic of the second-order FM-PM transition, which accords well with the case mentioned based on Fig. 2 where thermal hysteresis around  $T_{\text{C}}$  is absent.

The magnetic entropy change  $\Delta S$  of  $R_3\text{Ni}_2$  ( $R = \text{Ho}$  and  $\text{Er}$ ) compounds can be calculated from isothermal magnetization data by using Maxwell relation  $\Delta S = \int_0^H (\partial M / \partial T)_H dH$ . Figure 4(a) displays the values of  $\Delta S$  for  $R_3\text{Ni}_2$  ( $R = \text{Ho}$  and  $\text{Er}$ ) compounds as a function of temperature for the field changes of 0-2 T and 0-5 T. A broad cusp around  $T_{\text{SR}}$  is observed in each  $\Delta S$ - $T$  curve, which is in accord with the results of magnetic and specific capacity (see Fig. 4(b)) measurements. Another peak centers at  $T_{\text{C}}$  in every  $\Delta S$ - $T$  curve. For a field change of 0-5 T, the peak values of  $\Delta S$  for  $\text{Ho}_3\text{Ni}_2$  and  $\text{Er}_3\text{Ni}_2$  reach to  $21.7 \text{ J kg}^{-1} \text{ K}^{-1}$  and  $19.5 \text{ J kg}^{-1} \text{ K}^{-1}$ , respectively, which are comparable with or much larger than those of some magnetic refrigerant materials with a similar phase temperature, such as  $\text{DyNi}_2$  ( $21.3 \text{ J kg}^{-1} \text{ K}^{-1}$  at 20 K),<sup>18</sup>  $\text{DyCoAl}$  ( $16.3 \text{ J kg}^{-1} \text{ K}^{-1}$  at 37 K),<sup>19</sup>  $\text{HoNi}$  ( $14.5 \text{ J kg}^{-1} \text{ K}^{-1}$  at 36 K),<sup>13</sup>  $\text{TbCoC}_2$  ( $15.3 \text{ J kg}^{-1} \text{ K}^{-1}$  at 28 K),<sup>20</sup>  $\text{DyCuAl}$  ( $20.4 \text{ J kg}^{-1} \text{ K}^{-1}$  at 28 K),<sup>21</sup> and  $\text{ErGa}$  ( $21.3 \text{ J kg}^{-1} \text{ K}^{-1}$  at 30 K).<sup>22</sup>

One can find from Fig. 4(a) that the peak values of  $\Delta S$  around  $T_{\text{C}}$  for  $\text{Ho}_3\text{Ni}_2$  and  $\text{Er}_3\text{Ni}_2$  compounds approximately equal each other and the corresponding temperature span is only 17 K. So when  $\text{Ho}_3\text{Ni}_2$  and  $\text{Er}_3\text{Ni}_2$  compounds with the mass ratio of 2:3 are mixed together, the best quasi-platform

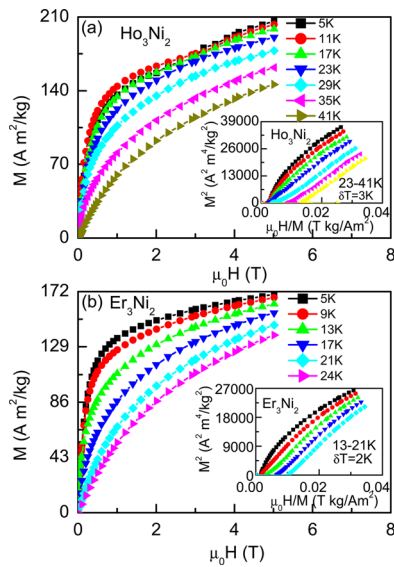


FIG. 3. (Color online) Typical magnetic isothermals of  $\text{Ho}_3\text{Ni}_2$  (a) and  $\text{Er}_3\text{Ni}_2$  (b) measured during field increasing. The insets of (a) and (b) show the Arrott-plots of  $\text{Ho}_3\text{Ni}_2$  and  $\text{Er}_3\text{Ni}_2$  around  $T_c$ , respectively.

of  $\Delta S$  is observed. The inset of Fig. 4(a) displays the temperature dependence of  $\Delta S$  for the composite material for a field change of 0-5 T. A large RC value of  $496 \text{ J kg}^{-1}$  is thus obtained, which is calculated by numerically integrating the area under the  $\Delta S$ - $T$  curve, with the temperatures at half maximum of the peak used as the integration limits.<sup>23</sup> The large RC attributes to the appreciably large values of  $\Delta S$  around  $T_c$  for  $R_3\text{Ni}_2$  ( $R = \text{Ho}$  and  $\text{Er}$ ) compounds.

In order to get better comprehension of the application potential of  $R_3\text{Ni}_2$  ( $R = \text{Ho}$  and  $\text{Er}$ ) compounds, we have also calculated the MCE in terms of adiabatic temperature change  $\Delta T_{\text{ad}}$  based on the data of Figs. 4(a) and 4(b) by using

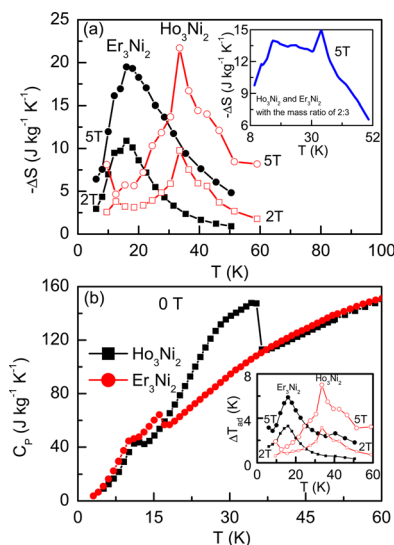


FIG. 4. (Color online) (a) Magnetic entropy change as a function of temperature for  $\text{Ho}_3\text{Ni}_2$  and  $\text{Er}_3\text{Ni}_2$  for magnetic field changes of 0-2 T and 0-5 T, where the inset shows the temperature dependence of magnetic entropy change for the composite material for a field change of 0-5 T. (b) Temperature dependences of the specific capacities for  $\text{Ho}_3\text{Ni}_2$  and  $\text{Er}_3\text{Ni}_2$  under zero field, where the inset shows the adiabatic temperature change curves for field changes of 0-2 T and 0-5 T.

$\Delta T_{\text{ad}} = -\Delta S(T, H) \times T / C_p(T, H_0)$ , where  $C_p(T, H_0)$  is zero-field specific heat. The inset of Fig. 4(b) shows the temperature dependences of  $\Delta T_{\text{ad}}$  of the  $\text{Ho}_3\text{Ni}_2$  and  $\text{Er}_3\text{Ni}_2$  compounds for field changes of 0-2 T and 0-5 T. The maximum values of  $\Delta T_{\text{ad}}$  are found to be 3.2 and 7.0 K for  $\text{Ho}_3\text{Ni}_2$ , 3.3 and 5.9 K for  $\text{Er}_3\text{Ni}_2$ , respectively. They are comparable well with those of  $\text{DyNi}_2$ ,<sup>18</sup>  $\text{DyCuAl}$ ,<sup>21</sup> and  $\text{DyNiAl}$ .<sup>24</sup>

In summary, from the magnetization and heat capacity measurements, it is found that  $R_3\text{Ni}_2$  ( $R = \text{Ho}$  and  $\text{Er}$ ) compounds undergo two successive phase transitions at low temperatures. Large  $\Delta S$  of  $21.7 \text{ J kg}^{-1} \text{K}^{-1}$  for  $\text{Ho}_3\text{Ni}_2$  and  $19.5 \text{ J kg}^{-1} \text{K}^{-1}$  for  $\text{Er}_3\text{Ni}_2$  are obtained for a field change of 0-5 T. The maximum values of  $\Delta T_{\text{ad}}$  for  $\text{Ho}_3\text{Ni}_2$  and  $\text{Er}_3\text{Ni}_2$  reach to 7.0 and 5.9 K for the same field change, respectively. For the composite material formed by  $\text{Ho}_3\text{Ni}_2$  and  $\text{Er}_3\text{Ni}_2$  with the mass ratio of 2:3, a large RC of  $496 \text{ J kg}^{-1}$  is achieved for a field change of 0-5 T. The excellent magnetocaloric properties indicate the applicability of  $R_3\text{Ni}_2$  ( $R = \text{Ho}$  and  $\text{Er}$ ) compounds to the liquefaction of hydrogen gas.

This work is supported by the National Natural Science Foundation of China (Grant Nos. 50731007, 11004204 and 51001077), the Hi-Tech Research and Development program of China, and the Knowledge Innovation Project of the Chinese Academy of Sciences.

- <sup>1</sup>W. F. Giauque and D. P. MacDougall, *Phys. Rev.* **43**, 0768 (1933).
- <sup>2</sup>A. H. Cooke, H. J. Duffus, and W. P. Wolf, *Philos. Mag.* **44**, 623 (1953).
- <sup>3</sup>A. M. Tishin and Y. I. Spichkin, in *The Magnetocaloric Effect and its Applications*, edited by J. M. D. Coey, D. R. Tilley, D. R. Vij (Institute of Physics Publishing, Bristol, 2003).
- <sup>4</sup>K. A. Gschneidner, V. K. Pecharsky, and A. O. Tsokol, *Rep. Prog. Phys.* **68**, 1479 (2005).
- <sup>5</sup>V. K. Pecharsky and K. A. Gschneidner, *Phys. Rev. Lett.* **78**, 4494 (1997).
- <sup>6</sup>F. X. Hu, B. G. Shen, J. R. Sun, and X. X. Zhang, *Chin. Phys.* **9**, 550 (2000).
- <sup>7</sup>F. X. Hu, B. G. Shen, J. R. Sun, Z. H. Cheng, G. H. Rao, and X. X. Zhang, *Appl. Phys. Lett.* **78**, 3675 (2001).
- <sup>8</sup>H. Wada and Y. Tanabe, *Appl. Phys. Lett.* **79**, 3302 (2001).
- <sup>9</sup>S. Gama, A. A. Coelho, A. de Campos, A. M. G. Carvalho, F. C. G. Gandra, P. J. von Ranke, and N. A. de Oliveira, *Phys. Rev. Lett.* **93**, 237202 (2004).
- <sup>10</sup>O. Tegus, E. Bruck, K. H. J. Buschow, and F. R. de Boer, *Nature (London)* **415**, 150 (2002).
- <sup>11</sup>F. X. Hu, B. G. Shen, and J. R. Sun, *Appl. Phys. Lett.* **76**, 3460 (2000).
- <sup>12</sup>N. V. Tristan, K. Nenkov, K. Skokova, and T. Palewski, *Physica B* **344**, 462 (2004).
- <sup>13</sup>P. Kumar, K. G. Suresh, A. K. Nigam, and O. Gutfleisch, *J. Phys. D: Appl. Phys.* **41**, 245006 (2008).
- <sup>14</sup>Y. Isikawa, K. Mori, K. Sato, M. Ohashi, and Y. Yamaguchi, *J. Appl. Phys.* **55**, 2031 (1984).
- <sup>15</sup>J. M. Moreau, D. Paccard, and D. Gignoux, *Acta Crystallogr.* **B30**, 2122 (1974).
- <sup>16</sup>J. M. Moreau, D. Paccard, and E. Parthe, *Acta Crystallogr.* **B30**, 2583 (1974).
- <sup>17</sup>A. Arrott, *Phys. Rev.* **108**, 1394 (1957).
- <sup>18</sup>P. J. von Ranke, V. K. Pecharsky, and K. A. Gschneidner, Jr., *Phys. Rev. B* **58**, 12110 (1998).
- <sup>19</sup>X. X. Zhang, F. W. Wang, and G. H. Wen, *J. Phys.: Condens. Matter* **13**, L747 (2001).
- <sup>20</sup>B. Li, J. Du, W. J. Ren, W. J. Hu, Q. Zhang, D. Li, and Z. D. Zhang, *Appl. Phys. Lett.* **92**, 242504 (2008).
- <sup>21</sup>Q. Y. Dong, B. G. Shen, J. Chen, J. Shen, and J. R. Sun, *J. Appl. Phys.* **105**, 113902 (2009).
- <sup>22</sup>J. Chen, B. G. Shen, Q. Y. Dong, F. X. Hu, and J. R. Sun, *Appl. Phys. Lett.* **95**, 132504 (2009).
- <sup>23</sup>K. A. Gschneidner, Jr., V. K. Pecharsky, A. O. Pecharsky, and C. B. Zimm, *Mater. Sci. Forum* **315-317**, 69 (1999).
- <sup>24</sup>N. K. Singh, K. G. Suresh, R. Nirmala, A. K. Nigam, and S. K. Malik, *J. Appl. Phys.* **99**, 08K904 (2006).